Published in final edited form as:
Neuroimage. 2009 March 1; 45(1): 10–16. doi:10.1016/j.neuroimage.2008.11.027.

Decreased white matter integrity in late-myelinating fiber pathways in Alzheimer's disease supports retrogenesis

N.H. Stricker[a], **B.C. Schweinsburg**[b,c], **L. Delano-Wood**[d,j], **C.E. Wierenga**[d,j], **K.J. Bangen**[e], **K.Y. Haaland**[a,f,g], **L.R. Frank**[h,j], **D.P. Salmon**[i], and **M.W. Bondi**[d,j,*]

[a] New Mexico VA Healthcare System, USA

[b] VA Connecticut Healthcare System, USA

[c] Yale University, USA

[d] Department of Psychiatry, University of California San Diego, School of Medicine, USA

[e] San Diego State University/University of California San Diego Joint Doctoral Program in Clinical Psychology, USA

[f] Department of Psychiatry, University of New Mexico, USA

[g] Department of Neurology, University of New Mexico, USA

[h] Department of Radiology, University of California San Diego, USA

[i] Department of Neurosciences, University of California San Diego, School of Medicine, USA

[j] VA San Diego Healthcare System, USA

Abstract

The retrogenesis model of Alzheimer's disease (AD) posits that white matter (WM) degeneration follows a pattern that is the reverse of myelogenesis. Using diffusion tensor imaging (DTI) to test this model, we predicted greater loss of microstructural integrity in late-myelinating WM fiber pathways in AD patients than in healthy older adults, whereas differences in early-myelinating WM fiber pathways were not expected. We compared 16 AD patients and 14 demographically-matched healthy older adults with a whole-brain approach via tract-based spatial statistics (TBSS), and a region of interest (ROI) approach targeting early-myelinating (posterior limb of internal capsule, cerebral peduncles) and late-myelinating (inferior longitudinal fasciculus [ILF], superior longitudinal fasciculus [SLF]) fiber pathways. Permutation-based voxelwise analysis supported the retrogenesis model. There was significantly lower fractional anisotropy (FA) in AD patients compared to healthy older adults in late-myelinating but not early-myelinating pathways. These group differences appeared to be driven by loss of myelin integrity based on our finding of greater radial diffusion in AD than in healthy elderly. ROI analyses were generally in agreement with whole-brain findings, with significantly lower FA and increased radial diffusion in the ILF in the AD group. Consistent with the retrogenesis model, AD patients showed demonstrable changes in late-myelinating WM fiber pathways. Given greater change in the ILF than the SLF, wallerian degeneration secondary to cortical atrophy may also be a contributing mechanism. Knowledge of the pattern of WM microstructural changes in AD and its underlying mechanisms may contribute to earlier detection and intervention in at-risk groups.

* Corresponding author. Psychology Service (116B), VA San Diego Healthcare System, 3350 La Jolla Village Drive, San Diego, CA 92161, USA. Fax: +1 858 642 1218. E-mail address: mbondi@ucsd.edu (M.W. Bondi).

Introduction

The retrogenesis model of Alzheimer's disease (AD) and other neurodegenerative diseases posits that white matter (WM) degeneration reflects myelin breakdown that develops in a pattern that is the reverse of myelogenesis (Reisberg et al., 1999). According to this model, pathways with large diameter fibers that myelinate first in development, such as primary motor fibers, are the last to be affected by AD. In contrast, pathways with small diameter fibers that myelinate much later in normal development, such as neocortical association and allocortical fibers, are the first to be affected by the AD degenerative process (Bartzokis, 2004). Because corticocortical association pathways are the latest-myelinating fiber pathways in the brain, followed by commissural and limbic pathways (Kinney et al., 1988; Yakovlev and Lecours, 1967), they are particularly vulnerable to early degeneration in AD according to the retrogenesis model. However, many of these late-myelinating pathways also connect to medial temporal lobe structures affected early in AD (Brun and Englund, 1986), so it is possible that observed WM changes may reflect wallerian degeneration secondary to neuronal loss as well (see Coleman, 2005).

Neuropathological mechanisms underlying WM changes in AD can be investigated using diffusion tensor imaging (DTI), which allows for *in vivo* examination of the orientation and microstructural integrity of WM. WM microstructural integrity is reflected by the degree of intravoxel diffusion anisotropy, most commonly represented as fractional anisotropy (FA, Le Bihan et al., 2001; Pierpaoli and Basser, 1996). Preliminary studies suggest that examination of directional diffusivities (e.g., axial and radial diffusion) may yield important information about the underlying neuropathology driving differences in FA (Song et al., 2003, 2002; Sun et al., 2005). Specifically, radial diffusion (DR) may signify loss of myelin integrity and axial diffusion (DA) may implicate axonal damage that would be expected with wallerian degeneration (Song et al., 2003, 2002; Sun et al., 2005).

Studies not specifically testing a theoretical model of WM changes in AD have provided mixed support for both the retrogenesis model and wallerian degeneration. Many published papers have attributed WM changes in late-myelinating or corticocortical pathways in AD to retrogenesis, but these studies did not directly compare early- versus late-myelinating regions (Fellgiebel et al., 2008; Naggara et al., 2006; Taoka et al., 2006; Teipel et al. 2007). For example, Teipel et al. (2007) used a whole-brain multivariate voxel-based morphometry (VBM) approach and found a pattern of regional WM changes consistent with the retrogenesis model. Specifically, patients with AD had significantly reduced FA in intracortical projecting WM tracts and a relative preservation of extracortical projecting fiber tracts. Other groups have concluded that their results support wallerian degeneration (Duan et al., 2006; Huang and Auchus, 2007; Yoshiura et al., 2006). For example, Huang and Auchus (2007) found decreased axial diffusivity in the temporal lobe in patients with AD or mild cognitive impairment (MCI) compared to healthy elderly, suggesting axonal damage secondary to wallerian degeneration. Other investigators have reported a pattern of results that support both wallerian degeneration and retrogenesis as possible neuropathological mechanisms of WM changes in AD (Medina et al., 2006; Salat et al., 2008; Stahl et al., 2007; Xie et al., 2006).

Although studies have consistently demonstrated reduced WM integrity in AD patients compared to healthy elderly, the pattern and underlying mechanism of these changes remain unclear. One reason for this uncertainty is that few studies have tested *a priori* hypotheses based on a specified neuropathological mechanism. The only study to date that tested the retrogenesis model prospectively used a region of interest (ROI) approach and found support for the model in AD (Choi et al., 2005). However, unlike the present study, these investigators did not additionally employ a whole-brain approach and their analyses were therefore limited to preselected ROIs.

In the present study we utilized a novel DTI post-processing procedure, tract-based spatial statistics (TBSS, Smith et al., 2006), to test the retrogenesis model of AD using both a whole-brain exploratory approach to evaluate regional patterns of WM changes and an ROI approach to test *a priori* hypotheses. We predicted that there would be less WM microstructural integrity in patients with AD relative to normal healthy elderly in late-myelinating WM fiber pathways, whereas early-myelinating fiber pathways would be relatively spared. We also investigated the underlying neuropathological mechanism of WM changes by testing whether group differences remained after controlling for generalized atrophy and by evaluating group differences in axial and radial diffusion. In accordance with the retrogenesis model, we predicted that group differences would be independent of generalized atrophy and would be driven by myelin breakdown rather than wallerian degeneration.

Method

Participants

The institutional review boards at the University of California San Diego and San Diego State University approved the study. Sixteen individuals diagnosed with possible or probable AD and 14 elderly normal control (NC) participants were selected for this study from the larger cohort of research volunteers of the Alzheimer's Disease Research Center (ADRC) at the University of California San Diego. The two groups did not differ significantly on age ($F_{1,28}$=.003, p=.96, η_p^2=.00), education ($F_{1,28}$=.25, p=.62, η_p^2=.01), or Rosen's Modified Hachinski Scale ($F_{1,28}$=.06, p=.80, η_p^2=.00). Sex (proportion) did not differ significantly across groups (χ^2=.53, p=.47). As expected, DRS total and MMSE scores for the AD group were significantly lower than for the NC group ($F_{1,28}$=69.64, p<.001, η_p^2=.71; $F_{1,28}$=26.31, p<.001, η_p^2=.48). Please see Table 1 for demographic descriptive statistics.

AD patients received a diagnosis of possible or probable AD by two senior staff neurologists according to the criteria developed by the National Institute of Neurological and Communicative Disorders and Stroke (NINCDS) and the Alzheimer's Disease and Related Disorders Association (McKhann et al., 1984). Individuals were excluded from the study if they had causes of dementia other than AD (e.g., stroke, hypothyroidism, vitamin B12 deficiency, electrolyte imbalance), a history of severe head injury, alcoholism, or serious psychiatric disturbance. Persons with significant cerebrovascular disease, (as indexed by modified Rosen ischemic scores greater than 4, Rosen et al., 1980), were excluded. All ADRC participants receive (a) annual neurological, medical, and psychiatric examinations; (b) global cognitive screening (e.g., Mattis Dementia Rating Scale, DRS, Mattis, 1976); and (c) the ADRC Core Neuropsychological Battery, which assesses basic cognitive domains such as attention, memory, language, visuospatial skill, problem solving and abstraction, and motor coordination. For a detailed description of the tests that comprise this battery, see Salmon and Butters (1992). Participants were scanned within 3.8 months, on average, of their ADRC annual evaluation (SD=2.2; range 0–9 months).

Imaging protocol

Participants were scanned in a 3-Tesla GE Signa Infinity MRI scanner equipped with quantum gradients providing echo planar capability. Automated shimming is used to enhance field homogeneity. We obtained both mid-sagittal and axial localizer slices to confirm the adequacy of head placement.

Structural MRI sequences were as follows:

1. T1: MPRAGE, TR=7 ms, TE=min full, flip angle=8°, inversion recovery prepared: inversion time 900 ms, bandwidth 31.25 kHz, FOV=26 cm, slice thickness=1.2 mm, Locs per slab=170, number of slabs=1, plane=sagittal, SPGR, freq=256, phase=256,

(matrix size 256×256), NEX=1, phase FOV=.94, frequency/direction=superior/inferior, auto center frequency=water, coil=8 channel phased array, scan time was approximately 9 min.

2. Two field maps were collected to correct for distortions in DTI images due to susceptibility artifact: TE=minimum full (1st field map) or 5.5 (2nd field map), TR=1,000 ms, FOV=24 cm, spacing=0, NEX=1, flip angle=60°, bandwidth =31.25 kHz, slice thickness= 3 mm, frequency=128, phase=128, phase fov=1, frequency/direction=1.

3. DTI images were collected in the axial plane with a double spin echo EPI acquisition (eddy current compensated), TR=11,000 ms, TE=minimum, FOV=24 cm, slice thickness=3 mm, spacing=0, matrix size 128×128, in-plane resolution=1.875×1.875. Approximately 36 slices were acquired with 15 non-collinear diffusion directions and 4 averages (*b* value=1500 s/mm^2). Total DTI acquisition time with field mapping was approximately 16 min.

Image processing

T1—Bias correction of field inhomogeneities was performed with N3 (Sled et al., 1998). The T1 images were skull stripped with Hybrid Watershed algorithm (Gootjes et al., 2004; Segonne et al., 2004), Brain Surface Extractor (BSE, Sandor and Leahy, 1997; Shattuck and Leahy, 2001), or both, as these two programs have been shown to be more effective than others (e.g., BET, 3dIntracranial) in patients with AD (Fennema-Notestine et al., 2006). Any remaining edits were performed manually.

Tissue segmentation was then performed using the Oxford Centre for Functional Magnetic Resonance Imaging of the BRAIN (FMRIB)'s Automated Segmentation Tool (FAST, Zhang et al., 2001) in order to derive gray matter (GM), white matter (WM), and cerebrospinal fluid (CSF) volumes. To correct for head size, GM volume was divided by the whole-brain volume (GM+WM+CSF) to generate proportionalized (e.g., percentage) GM volume.

DTI—Diffusion weighted images were submitted to FMRIB's Utility for Geometrically Unwarping EPIs (FUGUE) and Phase Region Expanding Labeller for Unwrapping Discrete Estimates (PRELUDE) programs, which unwarp echo-planar imaging (EPI) and DTI images to help correct phase variations in field map data due to field inhomogeneity and subtle subject movements. Next, eddy current correction was applied using the FMRIB's Software Library (FSL) program Eddy Correct to further adjust for the effects of head movement and eddy currents through affine registration. The 15 diffusion directions were registered to the B0 volume (e.g., no diffusion weighting) using FMRIB's Linear Image Registration Tool (FLIRT) with six degrees of freedom. The AFNI (Analysis of Functional NeuroImages) program 3dDWItoDT calculated the diffusion tensor from the diffusion weighted images using nonlinear estimation of the diffusion tensor model (Pierpaoli and Basser, 1996). Maps for FA (see Le Bihan et al., 2001 for formula), DA (λ_1), and DR ($\lambda_2+\lambda_3/2$) were then extracted to prepare for TBSS analysis.

Tract-based spatial statistics

Tract-based spatial statistics version 1.1 (TBSS, Smith et al., 2006), part of FSL (Smith et al., 2004), is a novel tool for the post-processing and analysis of multisubject DTI data. First, a target image was selected to serve as a target for all nonlinear registrations. As the target subject ideally is the “most typical” subject of the group, a normal control subject whose percentage brain volume (according to FAST segmentation) was at the median split for the entire sample was selected (per Smith et al., 2006, the final skeleton is quite comparable when different target subjects are used). All subjects' FA data were then aligned into a common space using the

nonlinear registration Image Registration Toolkit (IRTK, Rueckert et al., 1999) and then affine-transformed into 1×1×1 mm^3 MNI152 space. The aligned FA images were then averaged to create a mean FA image. The process of resolution upsampling and averaging across subjects rendered the mean FA image relatively smooth, obviating the need for additional smoothing. The mean FA image was subsequently thinned to create a mean FA skeleton by using a local search for each voxel in the tract perpendicular direction, identifying the voxel with the highest FA as the center of the tract. The resultant mean FA skeleton represents the central portion of all the fiber pathways throughout the brain that are common to the group. A threshold FA value of .2 was then applied to exclude voxels that are primarily GM or CSF. Each individual subject's aligned FA data was then probabilistically projected onto this skeleton using a searching algorithm. The same perpendicular tract direction that was used to create the original mean FA skeleton was used to search each individual's FA image to find the maximum FA value and assign this value to the skeleton voxel. Searching constraints ensure that the value assigned is closer to that skeleton voxel than any other part of the skeleton, with priority given to more proximate voxels (see Smith et al., 2006). In this way, each individual's FA skeleton should contain the center of their unique WM tracts, adjusted to the alignment of the group. The same transformations derived for the FA maps were applied to the DA and DR maps.

TBSS regions of interest

Regions of interest (ROIs) were created to represent two early-myelinating pathways and two late-myelinating pathways (see Fig. 1). The early-myelinating pathways included the posterior limb of the internal capsule (ICp) and the cerebral peduncles (CP). The late-myelinating pathways included the superior longitudinal fasciculus (SLF) and the inferior longitudinal fasciculus (ILF). ROIs were drawn on the mean FA skeleton (overlaid on mean FA map) and average FA values for each ROI were subsequently calculated for every subject. Two WM atlases within FSL (ICBM-DTI-81 parcellation map and JHU WM tractography atlas) guided the placement of the ROIs and they were further verified using a DTI color map human atlas (Mori et al., 2005) and a white matter atlas based on data from the rhesus monkey (Mori et al., 2005;Schmahmann and Pandya, 2006). Mori et al. (2008) reported that the ICBM-DTI-81 WM parcellation map serves as an effective guide for ROI drawing based upon high inter-rater reproducibility (κ>0.85). We also used these atlases to determine the location of significant voxels in the voxelwise group comparison. It should be noted that the ILF might also include voxels from the inferior fronto-occipital fasciculus (IFOF) because we defined the ILF using the ICBM-DTI-81 WM region labeled “sagittal stratum,” which did not differentiate between the ILF and IFOF. We chose to use the label ILF because Schmahmann and Pandya (2006) argue that an inferior fronto-occipital fasciculus is implausible and caution against propagation of this label.

Data analysis

To test for localized differences across groups, voxelwise statistics were performed for each point on the common FA skeleton. A permutation-based approach (Nichols and Holmes, 2001) that accounts for “familywise errors” was used to control for multiple comparisons. Specifically, permutation-based inference cluster size (t>1, p<.05) was used to test whether FA is significantly reduced in AD patients compared with NC participants. A mask of all significant voxels was created and submitted to a deprojection script within TBSS v1.1 to back-project all significant voxels into native FA spaces. This allowed for visual inspection of significant voxels to ensure that voxels fell within the WM pathways for each individual subject, and served as a method of checking the validity of the registration procedure.

An average FA, DA, and DR value was derived for the voxels on the skeleton that were significantly different across groups in the voxelwise analysis, and all were submitted to ANOVA to examine differences between groups and derive effect sizes (partial eta squared).

Any significant differences were then submitted to Analysis of Covariance (ANCOVA) to test whether these group differences remain when covarying for age and GM volume.

To test our *a priori* hypotheses about early- versus late-myelinating fiber pathways, an average FA was extracted for each ROI (e.g., SLF, ILF, CP, ICp) and aggregate early-myelinating FA (average of CP and ICp) and late-myelinating FA (average of SLF and ILF) values were calculated. A mixed model ANOVA was used to test whether there was a significant interaction of FA values between region (early- and late-myelinating) and group (NC and AD). This mixed-model ANOVA was then performed separately for each late-myelinating ROI. Differences in DA and DR were only examined if significant differences across groups were found in FA for an individual ROI. Because of the small sample size and the preliminary nature of this study, we did not control for multiple comparisons for the ROI analyses.

Results

Whole-brain voxelwise comparison

Voxelwise analyses revealed significantly lower FA values in AD patients compared to healthy older adults in late-myelinating association fiber pathways (uncinate fasciculus, ILF, SLF), limbic pathways (fornix/stria terminalus, cingulum), and commissural pathways (splenium of the corpus callosum, forceps major). In contrast, no significant differences were seen in early-myelinating pathways (e.g. cerebral peduncles, internal capsule, corona radiata). See Fig. 2.

In order to more specifically identify the constituents impacting the previous results, we analyzed group differences in FA, DA, and DR for the voxels that showed significant group differences in the previous analysis. The AD group showed significantly lower FA ($F_{1,28}$= 17.69, p<.001, η_p^2=.39) and higher DR ($F_{1,28}$=9.48, p=.005, η_p^2=.25) than the NC group. There was no significant difference in DA across groups ($F_{1,28}$=.00, p=.96, η_p^2=.00). The group differences in FA and DR remained significant when controlling for age and GM volume ($F_{1,26}$=19.55, p<.001, η_p^2=.43, and $F_{1,26}$=7.26, p=.01, η_p^2=.22, respectively) (Table 2).

ROI group comparisons

No significant differences in FA across groups were found in aggregate early-myelinating regions (internal capsule, cerebral peduncles; $F_{1,28}$=0.32, p=.58, η_p^2=.01). A significant difference in FA was found for aggregate late-myelinating regions (ILF, SLF; $F_{1,28}$=4.49, p=. 04, η_p^2= .14), with the AD group showing lower FA than the NC group. When the two late-myelinating ROIs were tested separately, the ILF showed a significant difference in FA ($F_{1,28}$=6.15, p=.02, η_p^2= .18), again with the AD group showing lower FA than the NC group, but the SLF did not ($F_{1,28}$=.74, p=.40, η_p^2=.03). See Table 3 for descriptive statistics. Because of the significant difference in FA across groups in the ILF, directional diffusivities were also tested. DR of the ILF was greater for the AD group than the NC group and this difference approached significance ($F_{1,28}$=3.75, p=.06, η_p^2= .12). DA of the ILF was not significantly different across groups ($F_{1,28}$=.01, p=.93, η_p^2=.00).

A mixed-model ANOVA was performed to test for an interaction of the within-subjects factor (region: early vs. late) and the between-subjects factor (group: NC vs. AD). When testing the aggregate ROI results of early- versus late-myelinating regions, the region (early/late) by group (NC/AD) interaction approached significance ($F_{1,28}$=2.81, p=.11, η_p^2=.09). This mixed-model ANOVA was then performed separately for each late-myelinating ROI. For the SLF, the region (early/SLF) by group (NC/AD) interaction was not significant ($F_{1,28}$= .13, p=.72, η_p^2=.01). For the ILF, the region (early/ILF) by group (NC/AD) interaction was significant ($F_{1,28}$=4.28, p=.05, η_p^2= .13; see Table 3 for descriptive statistics).

Discussion

The present DTI study used TBSS to test the retrogenesis model of AD using both a whole brain voxelwise approach and *a priori* ROI analyses. Generally, our preliminary findings are consistent with the retrogenesis model, although wallerian degeneration due to cortical atrophy cannot be fully ruled out as a mechanism of WM change.

Whole brain voxelwise analysis

Consistent with the retrogenesis model of WM degeneration in AD, we found abnormally low WM integrity in AD patients in corticocortical association pathways (uncinate fasciculus, inferior longitudinal fasciculus, and superior longitudinal fasciculus), commissural pathways (splenium, forceps major), and limbic pathways (fornix/stria terminalus, cingulum). These are among the latest-myelinating pathways in the brain (Kinney et al., 1988; Yakovlev and Lecours, 1967). Early-myelinating fiber pathways associated with primary motor and sensory regions, as predicted, were spared in early AD. These results are consistent with those of Teipel et al. (2007) who used a multivariate approach (principle components analysis) with VBM to examine differences in FA across AD and NC groups. They are also consistent with those of Damoiseaux et al. (2008) who employed TBSS for voxelwise analysis to show significantly lower FA in the left uncinate fasciculus in AD patients. It should be noted, however, that abnormally low FA was observed in many more late-myelinating regions in the present study than in the Damoiseaux et al. (2008) study, perhaps because the AD and NC participants were seven years older, on average, than those studied by Damoiseaux et al. In addition, there was nearly twice as much variability in mean FA skeleton values for the healthy elderly group than for the AD group in the Damoiseaux et al. (2008) study, which may have made meaningful group differences difficult to detect.

Although the voxelwise analysis results are consistent with retrogenesis, possible contributions from wallerian degeneration to WM changes in AD cannot be ruled out. The ILF, splenium, fornix/stria terminalus, and cingulum fiber pathways all have connections to brain structures (e.g., medial temporal lobe structures such as the hippocampal formation) affected early in the course of AD (Braak and Braak, 1996) and changes in these structures could lead to wallerian degeneration (Coleman, 2005). Arguing against this possibility, however, is our finding that radial diffusion, a reflection of loss of myelin integrity, rather than axial diffusion, a reflection of wallerian degeneration, revealed reduced FA in patients with AD compared to NC subjects. Furthermore, group differences in FA remained significant after covarying for age and GM volume, which suggests that the observed changes in WM integrity cannot be entirely explained by GM loss. Similar results were reported by Salat et al. (2008) who found greater changes in radial rather than axial diffusion in medial temporal lobe WM after controlling for hippocampal volume. If wallerian degeneration were the primary mechanism of WM change in AD, variance due to GM atrophy would be expected to at least partially account for the change in microstructural WM integrity. Thus, the abnormalities in WM we observed in patients with AD appear to be related to alterations of the integrity of myelin (Song et al., 2005), which is more in accordance with retrogenesis through mechanisms outlined by Bartzokis (2004) than with wallerian degeneration secondary to distal GM atrophy. This interpretation is consistent with Brun and Englund (1986) neuropathological findings, which indicated that white matter changes in AD are not likely to be solely due to wallerian degeneration.

ROI analyses

Results from our ROI analyses provide mixed support for the retrogenesis model. Consistent with the model and a number of previous studies (Naggara et al., 2006; Rose et al., 2000, 2008; Xie et al., 2006; Zhang et al., 2007), there were no significant differences between AD patients and healthy elderly in early-myelinating regions such as the cerebral peduncles or the

posterior limb of the internal capsule. Furthermore, patients with AD had decreased WM integrity compared to normal healthy elderly across late-myelinating pathways as predicted by the retrogenesis model. However, when the late-myelinating ILF and SLF were separately evaluated, it became clear that the group difference was driven almost entirely by changes in the ILF. There was a significant region (early- versus late-myelinating) by group interaction effect when the ILF represented the late-myelinating region, but not when the late-myelinating region was represented by the SLF. These results are consistent with a recent study by Fellgiebel et al. (2008) who also failed to find group differences in early AD patients compared to normal healthy elderly in the SLF when using an ROI approach.

Because the ILF contains connections between medial temporal lobe areas affected early in the AD neuropathological process (Braak and Braak, 1996) and posterior cortical regions, it is possible that the observed group differences in this fiber pathway could be explained by wallerian degeneration. In contrast, the SLF primarily connects the frontal and parietal lobes (Schmahmann and Pandya, 2006), which are affected later in the disease process than medial temporal lobe structures (Braak and Braak, 1996). Therefore, WM changes due to wallerian degeneration are more likely in the ILF than the SLF in our sample of mildly-to-moderately impaired AD patients. Although wallerian degeneration cannot be ruled out, our finding that radial diffusion and not axial diffusion reveals decreased WM integrity in the ILF in our AD group argues against its importance.

Discrepancies in the literature and the retrogenesis model

Our findings have implications for discrepancies in the literature that relate to the issue of greater anterior versus posterior WM changes in AD. Although a number of investigators using DTI report that WM changes in AD patients are found predominantly in anterior regions (Choi et al., 2005; Duan et al., 2006; Naggara et al., 2006), other investigators using this procedure report that WM changes occur predominantly in posterior regions (Head et al., 2004; Medina et al., 2006; Rose et al., 2000; Takahashi et al., 2002). Our results indicate that WM in both anterior and posterior regions is affected in AD, but the important distinction is not its location, but whether the region is early- or late-myelinating. This perspective suggests that an alternative, and perhaps more unifying, approach to characterizing the pattern of WM degeneration in AD is to predict WM changes in vulnerable late-myelinating fiber pathways, rather than looking for anterior versus posterior gradients of change (see Salat et al., 2005 for a similar approach in normal aging). A general principle that may guide this approach is that myelination of functional systems that are critical early in life (e.g., sensorimotor systems) begins earlier and progresses more rapidly than myelination of functional systems that are not necessary until later in childhood and have a higher evolutionary function (e.g., language, executive functions Barkovich, 2005; Yakovlev and Lecours, 1967). This sequence is consistent with the progression of cognitive changes in AD (e.g., relative preservation of sensory and motor functions in the presence of memory, language and executive function deficits) and is consistent with the retrogenesis model of WM change in AD.

Limitations and future directions

Although our study was limited by a relatively small sample size, a problem common to most neuroimaging studies of this kind, we were able to detect group differences in WM integrity that were congruent with our *a priori* hypotheses and with the extant literature. Our results suggest that retrogenesis may be the primary mechanism of WM change in mild to moderate AD patients. However, without longitudinal data and measures of cortical gray matter structures thought to be affected prior to these WM pathways, the primacy of GM atrophy cannot be determined. Although the current study focused on the retrogenesis model in subjects with AD, this model may be applicable to a number of neurodegenerative processes as suggested by Bartzokis (2004). Future studies should include other types of degenerative

syndromes to help elucidate whether the process of retrogenesis is specific to AD or if it represents a more general neurodegenerative process.

Another limitation is that while TBSS circumvents some of the problems with VBM that can lead to partial voluming, these problems remain when examining smaller WM tracts. In particular, if the tract width is smaller than the original voxel size, the voxel may include GM (Smith et al., 2006). We attempted to minimize this potential problem by applying an initial threshold that removes all voxels with an FA value less than .2, but care should be taken when interpreting group differences in small WM tracts (e.g., the fornix). Variability in registration procedures may lead to differing results across studies, thus replication of these results in native space and with other registration procedures such as TBSS v1.2 is needed.

Finally, it is possible that differences in WM integrity that we observed across groups could be related to factors other than AD pathology, such as subtle registration error or cerebrovascular disease (Delano-Wood et al., in press). The AD patients and healthy control subjects did not differ significantly in stroke risk measured by the Hachinski ischemia score, but this does not guarantee that vascular processes did not underlie some of the results. The relationship between WM microstructural integrity and vascular risk factors warrants further study and may prove to be a moderating factor in the development of AD or in disease expression. Future longitudinal studies of groups at risk for AD that implement a broader range of stroke risk or incorporate multiple imaging modalities that directly assess perfusion rates or stenosis of the vasculature will best address this issue.

Summary

Our prospective DTI study demonstrated that patients with AD show changes in late-myelinating WM fiber pathways consistent with the retrogenesis model of neurodegeneration. Although some contribution of wallerian degeneration to this model of WM change cannot be ruled out, the observed group differences remained even when controlling for GM volume, suggesting that DTI captures unique variance associated with neurodegenerative brain changes that traditional structural MR measures may miss. Knowledge of the pattern of WM microstructural changes in AD and its underlying mechanisms may contribute to earlier detection and intervention in groups at risk for AD, especially if WM abnormalities are not entirely due to changes in cortical volume.

Acknowledgments

This work was supported by grants from the National Institutes of Health (NIMH T32 MH019934, NINDS F31 NS059193, NIA P50 AG005131, NIA RO1 AG012674, NIA K24 AG026431, NIH 5 R01 MH64729-05, NIH 5 R01 MH075870-02) and from the Alzheimer's Association (IIRG-07-59343). The content is solely the responsibility of the authors and does not necessarily represent the official views of the National Institutes of Health or the Alzheimer's Association. The authors gratefully acknowledge the assistance of staff, patients, and volunteers of the UCSD Alzheimer's Disease Research Center, and the UCSD Laboratory of Cognitive Imaging.

References

Barkovich AJ. Magnetic resonance techniques in the assessment of myelin and myelination. J Inherit Metab Dis 2005;28:311–343. [PubMed: 15868466]

Bartzokis G. Age-related myelin breakdown: a developmental model of cognitive decline and Alzheimer's disease. Neurobiol Aging 2004;25:5–18. [PubMed: 14675724]author reply 49–62

Braak H, Braak E. Evolution of the neuropathology of Alzheimer's disease. Acta Neurol Scand 1996;165 (Suppl):3–12.

Brun A, Englund E. A white matter disorder in dementia of the Alzheimer type: a pathoanatomical study. Ann Neurol 1986;19:253–262. [PubMed: 3963770]

Choi SJ, Lim KO, Monteiro I, Reisberg B. Diffusion tensor imaging of frontal white matter microstructure in early Alzheimer's disease: a preliminary study. J Geriatr Psychiatry Neurol 2005;18:12–19. [PubMed: 15681623]

Coleman M. Axon degeneration mechanisms: commonality amid diversity. Nat Rev Neurosci 2005;6:889–898. [PubMed: 16224497]

Damoiseaux JS, Smith SM, Witter MP, Arigita EJ, Barkhof F, Scheltens P, Stam CJ, Zarei M, Rombouts SA. White matter tract integrity in aging and Alzheimer's disease. Hum Brain Mapp. 200810.1002/hbm.20563

Delano-Wood L, Bondi MW, Jak AJ, Stricker NH, Schweinsburg BC, Frank LR, Wierenga CE, Delis DC, Thielmann RJ, Salmon DP. Stroke risk modifies regional white matter differences in mild cognitive impairment. Neurobiol Aging. 10.1016/j.neurobiolaging.2008.09.013in press

Duan JH, Wang HQ, Xu J, Lin X, Chen SQ, Kang Z, Yao ZB. White matter damage of patients with Alzheimer's disease correlated with the decreased cognitive function. Surg Radiol Anat 2006;28:150–156. [PubMed: 16614789]

Fellgiebel A, Schermuly I, Gerhard A, Keller I, Albrecht J, Weibrich C, Muller MJ, Stoeter P. Functional relevant loss of long association fibre tracts integrity in early Alzheimer's disease. Neuropsychologia 2008;46:1698–1706. [PubMed: 18243252]

Fennema-Notestine C, Ozyurt IB, Clark CP, Morris S, Bischoff-Grethe A, Bondi MW, Jernigan TL, Fischl B, Segonne F, Shattuck DW, Leahy RM, Rex DE, Toga AW, Zou KH, Brown GG. Quantitative evaluation of automated skull-stripping methods applied to contemporary and legacy images: effects of diagnosis, bias correction, and slice location. Hum Brain Mapp 2006;27:99–113. [PubMed: 15986433]

Gootjes L, Teipel SJ, Zebuhr Y, Schwarz R, Leinsinger G, Scheltens P, Moller HJ, Hampel H. Regional distribution of white matter hyperintensities in vascular dementia, Alzheimer's disease and healthy aging. Dement Geriatr Cogn Disord 2004;18:180–188. [PubMed: 15211074]

Head D, Buckner RL, Shimony JS, Williams LE, Akbudak E, Conturo TE, McAvoy M, Morris JC, Snyder AZ. Differential vulnerability of anterior white matter in nondemented aging with minimal acceleration in dementia of the Alzheimer type: evidence from diffusion tensor imaging. Cereb Cortex 2004;14:410–423. [PubMed: 15028645]

Huang J, Auchus AP. Diffusion tensor imaging of normal appearing white matter and its correlation with cognitive functioning in mild cognitive impairment and Alzheimer's disease. Ann N Y Acad Sci 2007;1097:259–264. [PubMed: 17413027]

Kinney HC, Brody BA, Kloman AS, Gilles FH. Sequence of central nervous system myelination in human infancy. II. Patterns of myelination in autopsied infants. J Neuropathol Exp Neurol 1988;47:217–234. [PubMed: 3367155]

Le Bihan D, Mangin JF, Poupon C, Clark CA, Pappata S, Molko N, Chabriat H. Diffusion tensor imaging: concepts and applications. J Magn Reson Imaging 2001;13:534–546. [PubMed: 11276097]

Mattis, S. Dementia Rating Scale Professional Manual Psychological Assessment Resources. Odessa: 1976.

McKhann G, Drachman D, Folstein M, Katzman R, Price D, Stadlan EM. Clinical diagnosis of Alzheimer's disease: report of the NINCDS-ADRDA Work Group under the auspices of Department of Health and Human Services Task Force on Alzheimer's Disease. Neurology 1984;34:939–944. [PubMed: 6610841]

Medina D, DeToledo-Morrell L, Urresta F, Gabrieli JD, Moseley M, Fleischman D, Bennett DA, Leurgans S, Turner DA, Stebbins GT. White matter changes in mild cognitive impairment and AD: a diffusion tensor imaging study. Neurobiol Aging 2006;27:663–672. [PubMed: 16005548]

Mori, S.; Wakana, S.; Nagae-Poetscher, LM.; van Zijl, PCM. MRI Atlas of Human White Matter. Elsevier B. V.; Amsterdam: 2005.

Mori S, Oishi K, Jiang H, Jiang L, Li X, Akhter K, Hua K, Faria AV, Mahmood A, Woods R, Toga AW, Pike GB, Neto PR, Evans A, Zhang J, Huang H, Miller MI, van Zijl P, Mazziotta J. Stereotaxic white matter atlas based on diffusion tensor imaging in an ICBM template. NeuroImage 2008;40:570–582. [PubMed: 18255316]

Naggara O, Oppenheim C, Rieu D, Raoux N, Rodrigo S, Dalla Barba G, Meder JF. Diffusion tensor imaging in early Alzheimer's disease. Psychiatry Res 2006;146:243–249. [PubMed: 16520023]

Nichols TE, Holmes AP. Nonparametric permutation tests for functional neuroimaging: a primer with examples. Hum Brain Mapp 2001;15:1–25. [PubMed: 11747097]

Pierpaoli C, Basser PJ. Toward a quantitative assessment of diffusion anisotropy. Magn Reson Med 1996;36:893–906. [PubMed: 8946355]

Reisberg B, Franssen EH, Hasan SM, Monteiro I, Boksay I, Souren LE, Kenowsky S, Auer SR, Elahi S, Kluger A. Retrogenesis: clinical, physiologic, and pathologic mechanisms in brain aging, Alzheimer's and other dementing processes. Eur Arch Psychiatry Clin Neurosci 1999;249(Suppl 3):28–36. [PubMed: 10654097]

Rose SE, Chen F, Chalk JB, Zelaya FO, Strugnell WE, Benson M, Semple J, Doddrell DM. Loss of connectivity in Alzheimer's disease: an evaluation of white matter tract integrity with colour coded MR diffusion tensor imaging. J Neurol Neurosurg Psychiatry 2000;69:528–530. [PubMed: 10990518]

Rose SE, Janke AL, Chalk JB. Gray and white matter changes in Alzheimer's disease: a diffusion tensor imaging study. J Magn Reson Imaging 2008;27:20–26. [PubMed: 18050329]

Rosen WG, Terry RD, Fuld PA, Katzman R, Peck A. Pathological verification of ischemic score in differentiation of dementias. Ann Neurol 1980;7:486–488. [PubMed: 7396427]

Rueckert D, Sonoda LI, Hayes C, Hill DL, Leach MO, Hawkes DJ. Nonrigid registration using free-form deformations: application to breast MR images. IEEE Trans Med Imag 1999;18:712–721.

Salat DH, Tuch DS, Greve DN, van der Kouwe AJ, Hevelone ND, Zaleta AK, Rosen BR, Fischl B, Corkin S, Rosas HD, Dale AM. Age-related alterations in white matter microstructure measured by diffusion tensor imaging. Neurobiol Aging 2005;26:1215–1227. [PubMed: 15917106]

Salat DH, Tuch DS, van der Kouwe AJ, Greve DN, Pappu V, Lee SY, Hevelone ND, Zaleta AK, Growdon JH, Corkin S, Fischl B, Rosas HD. White matter pathology isolates the hippocampal formation in Alzheimer's disease. Neurobiol Aging. 200810.1016/j.neurobiolaging.2008.03.013

Salmon, DP.; Butters, N. Neuropsychological assessment of dementia in the elderly. In: Katzman, R.; Rowe, JW., editors. Principles of Geriatric Neurology. F. A. Davis; Philadelphia: 1992. p. 144-163.

Sandor S, Leahy R. Surface-based labeling of cortical anatomy using a deformable atlas. IEEE Trans Med Imag 1997;16:41–54.

Schmahmann, JD.; Pandya, DN. Fiber Pathways of the Brain. University Press; Oxford: 2006.

Segonne F, Dale AM, Busa E, Glessner M, Salat D, Hahn HK, Fischl B. A hybrid approach to the skull stripping problem in MRI. NeuroImage 2004;22:1060–1075. [PubMed: 15219578]

Shattuck DW, Leahy RM. Automated graph-based analysis and correction of cortical volume topology. IEEE Trans Med Imag 2001;20:1167–1177.

Sled JG, Zijdenbos AP, Evans AC. A nonparametric method for automatic correction of intensity nonuniformity in MRI data. IEEE Trans Med Imag 1998;17:87–97.

Smith SM, Jenkinson M, Woolrich MW, Beckmann CF, Behrens TE, Johansen-Berg H, Bannister PR, De Luca M, Drobnjak I, Flitney DE, Niazy RK, Saunders J, Vickers J, Zhang Y, De Stefano N, Brady JM, Matthews PM. Advances in functional and structural MR image analysis and implementation as FSL. NeuroImage 2004;23(Suppl 1):S208–219. [PubMed: 15501092]

Smith SM, Jenkinson M, Johansen-Berg H, Rueckert D, Nichols TE, Mackay CE, Watkins KE, Ciccarelli O, Cader MZ, Matthews PM, Behrens TE. Tract-based spatial statistics: voxelwise analysis of multi-subject diffusion data. NeuroImage 2006;31:1487–1505. [PubMed: 16624579]

Song SK, Sun SW, Ramsbottom MJ, Chang C, Russell J, Cross AH. Dysmyelination revealed through MRI as increased radial (but unchanged axial) diffusion of water. NeuroImage 2002;17:1429–1436. [PubMed: 12414282]

Song SK, Sun SW, Ju WK, Lin SJ, Cross AH, Neufeld AH. Diffusion tensor imaging detects and differentiates axon and myelin degeneration in mouse optic nerve after retinal ischemia. NeuroImage 2003;20:1714–1722. [PubMed: 14642481]

Song SK, Yoshino J, Le TQ, Lin SJ, Sun SW, Cross AH, Armstrong RC. Demyelination increases radial diffusivity in corpus callosum of mouse brain. NeuroImage 2005;26:132–140. [PubMed: 15862213]

Stahl R, Dietrich O, Teipel SJ, Hampel H, Reiser MF, Schoenberg SO. White matter damage in Alzheimer disease and mild cognitive impairment: assessment with diffusion-tensor MR imaging and parallel imaging techniques. Radiology 2007;243:483–492. [PubMed: 17456872]

Sun SW, Song SK, Harms MP, Lin SJ, Holtzman DM, Merchant KM, Kotyk JJ. Detection of age-dependent brain injury in a mouse model of brain amyloidosis associated with Alzheimer's disease using magnetic resonance diffusion tensor imaging. Exp Neurol 2005;191:77–85. [PubMed: 15589514]

Takahashi S, Yonezawa H, Takahashi J, Kudo M, Inoue T, Tohgi H. Selective reduction of diffusion anisotropy in white matter of Alzheimer disease brains measured by 3.0 Tesla magnetic resonance imaging. Neurosci Lett 2002;332:45–48. [PubMed: 12377381]

Taoka T, Iwasaki S, Sakamoto M, Nakagawa H, Fukusumi A, Myochin K, Hirohashi S, Hoshida T, Kichikawa K. Diffusion anisotropy and diffusivity of white matter tracts within the temporal stem in Alzheimer disease: evaluation of the “tract of interest” by diffusion tensor tractography. AJNR Am J Neuroradiol 2006;27:1040–1045. [PubMed: 16687540]

Teipel SJ, Stahl R, Dietrich O, Schoenberg SO, Perneczky R, Bokde ALW, Reiser MF, Moller HJ, Hampel H. Multivariate network analysis of fiber tract integrity in Alzheimer's disease. NeuroImage 2007;34:985–995. [PubMed: 17166745]

Xie S, Xiao JX, Gong GL, Zang YF, Wang YH, Wu HK, Jiang XX. Voxel-based detection of white matter abnormalities in mild Alzheimer disease. Neurology 2006;66:1845–1849. [PubMed: 16801648]

Yakovlev, PI.; Lecours, AR. The myelogenetic cycles of regional maturation of the brain. In: Minkowski, A., editor. Regional Development of the Brain in Early Life. F. A. Davis Company; Philadelphia: 1967. p. 3-70.

Yoshiura T, Mihara F, Koga H, Ohyagi Y, Noguchi T, Togao O, Ogomori K, Miyoshi K, Yamasaki T, Kaneko K, Ichimiya A, Kanba S, Honda H. Mapping of subcortical white matter abnormality in Alzheimer's disease using diffusion-weighted magnetic resonance imaging. Acad Radiol 2006;13:1460–1464. [PubMed: 17138113]

Zhang Y, Brady M, Smith S. Segmentation of brain MR images through a hidden Markov random field model and the expectation-maximization algorithm. IEEE Trans Med Imag 2001;20:45–57.

Zhang Y, Schuff N, Jahng GH, Bayne W, Mori S, Schad L, Mueller S, Du AT, Kramer JH, Yaffe K, Chui H, Jagust WJ, Miller BL, Weiner MW. Diffusion tensor imaging of cingulum fibers in mild cognitive impairment and Alzheimer disease. Neurology 2007;68:13–19. [PubMed: 17200485]

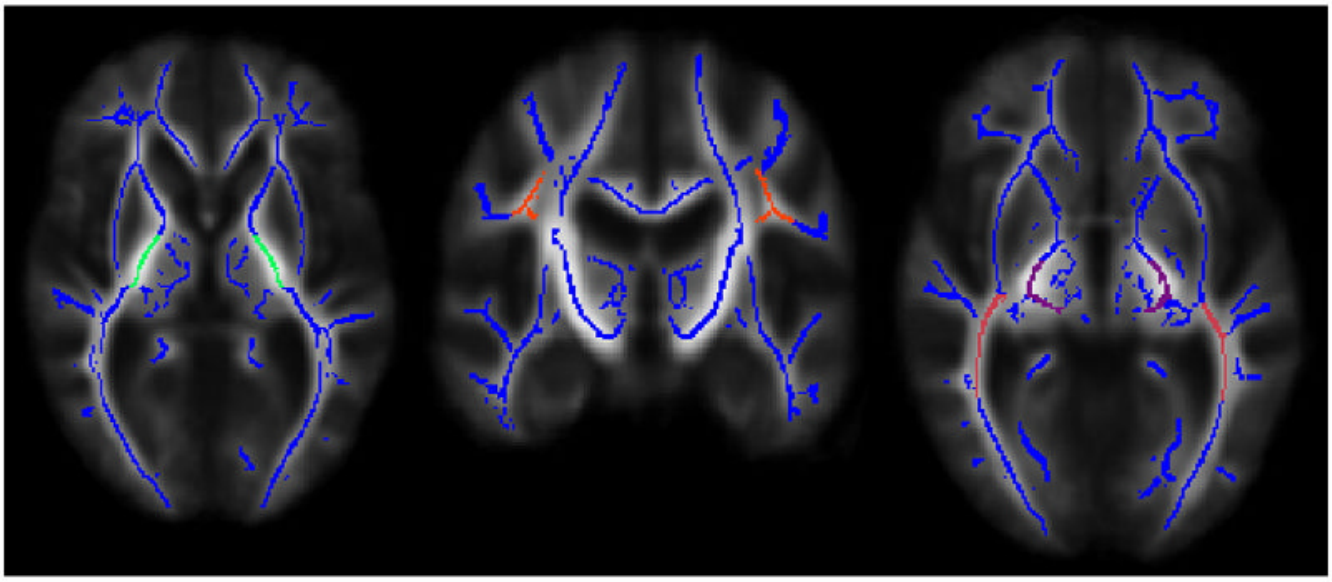

Fig. 1.
Regions of interest: posterior limb of the internal capsule (in green), superior longitudinal fasciculus (in orange), cerebral peduncles (in purple), and inferior longitudinal fasciculus (in pink) overlaid on mean FA skeleton (in blue). The left hemisphere of the brain corresponds to the right side of the image.

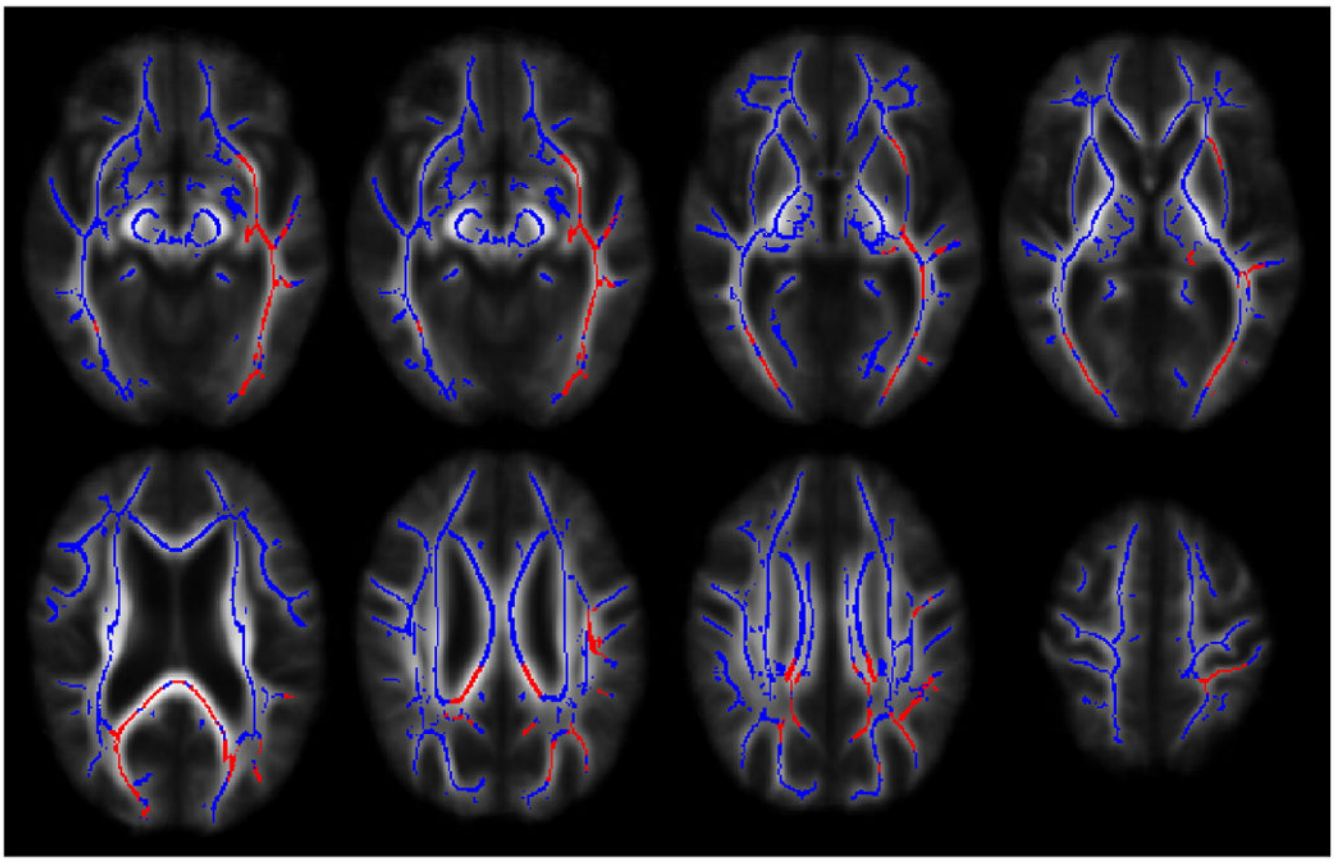

Fig. 2.
Voxelwise group differences in the uncinate fasciculus, inferior longitudinal fasciculus, fornix, splenium, cingulum, forceps major and superior longitudinal fasciculus (in red) overlaid on mean FA skeleton (in blue). In all instances, AD patients demonstrated significantly lower fractional anisotropy values in the aforementioned regions. The left hemisphere of the brain corresponds to the right side of the image.

Table 1

Demographic data for Alzheimer's disease (AD) patients and healthy normal control (NC) participants[a]

	NC *n* = 14	AD *n* = 16
Age	77.4 (8.1)	77.3 (9.0)
Education	15.3 (2.9)	15.8 (2.1)
Sex % female (M/F)	64% (5/9)	50% (8/8)
Rosen's Modified Hachinski Scale	0.36 (0.50)	0.31 (0.48)
Mattis Dementia Rating Scale[b]	141.1 (4.0)	124.0 (6.7)
Mini-Mental State Exam[b]	29.29 (.73)	24.44 (3.46)

[a] Mean (SD).

[b] $p<.05$.

Table 2

Group comparisons of average diffusion measures and brain volume indices in patients with Alzheimer's disease (AD) and healthy normal control (NC) participants[a]

	NC *n* = 14	AD *n* = 16	*p*
FA[b]	.445 (.033)	.399 (.027)	<.001
DA	1.565 (.064)	1.566 (.057)	.96
DR[b]	.742 (.074)	.817 (.060)	.005
Gray matter (%)	.444 (.031)	.425 (.021)	.07

Note. FA=FA skeleton voxels that were significantly different across groups in FA voxelwise analysis, DA=DA skeleton voxels that were significantly different across groups in FAvoxelwise analysis, DR=DR skeleton voxels that were significantly different across groups in FA voxelwise analysis.

[a] Mean (SD).

[b] $p<.01$.

Table 3

Average fractional anisotropy values for Alzheimer's disease (AD) patients and healthy normal control (NC) participants for each region of interest[a]

	NC *n* = 14	AD *n* = 16	*p*
Early-myelinating	.644 (.023)	.638 (.031)	.58
CP	.620 (.026)	.617 (.029)	.75
ICp	.667 (.028)	.659 (.039)	.52
Late-myelinating[b]	.435 (.027)	.414 (.028)	.04
SLF	.403 (.027)	.394 (.030)	.40
ILF[b]	.467 (.036)	.434 (.037)	.02

Note. CP=cerebral peduncles, ICp=posterior limb of the internal capsule, SLF=superior longitudinal fasciculus, ILF=inferior longitudinal fasciculus.

[a] Mean (SD).

[b] $p<.05$.